

1 **Diversity in the Utilization of Different Molecular Classes of** 2 **Dissolved Organic Matter by Heterotrophic Marine Bacteria**

3 Shira Givati* (1, 2), Elena Forchielli* (3), Dikla Aharonovich (1), Noga Barak (1), Osnat
4 Weissberg (1), Natalia Belkin (2), Eyal Rahav (2), Daniel Segrè (3, 4), Daniel Sher (1)#

5 * Equal contribution

6 (1) Department of Marine Biology, University of Haifa, Haifa, Israel

7 (2) Israel Oceanographic and Limnological Research, National Institute of Oceanography, Tel Shikmona, P.O. Box
8 8030, Haifa 31080, Israel

9 (3) Department of Biology, Boston University, Boston, Massachusetts, USA

10 (4) Department of Biomedical Engineering, Department of Physics, Biological Design Center, Boston University,
11 Boston, Massachusetts, USA

12 # Corresponding author: dsher@univ.haifa.ac.il

13 **Running title:** Marine community response to molecular classes of DOM

14

15 **Abstract**

16 Heterotrophic marine bacteria utilize and recycle dissolved organic matter (DOM), impacting
17 biogeochemical cycles. It is currently unclear to what extent distinct DOM components can be
18 utilized by different heterotrophic clades. Here, we ask how a natural microbial community from
19 the Eastern Mediterranean Sea responds to different molecular classes of DOM. These molecular
20 classes - peptides, amino acids, amino sugars, disaccharides, monosaccharides and organic acids
21 - together comprise much of the biomass of living organisms, released upon their death as DOM.

22 Bulk bacterial activity increased after 24-hours for all treatments relative to the control, while
23 glucose and ATP uptake decreased or remained unchanged. The relative abundance of several
24 bacterial families, assessed using 16S rRNA amplicon sequencing, increased in some treatments:
25 peptides promoted an increase in *Pseudoalteromonadaceae*, disaccharides promoted both
26 *Pseudoalteromonadaceae* and *Alteromonadaceae*, and most other treatments were dominated by
27 *Vibrionaceae*. While some results were consistent with recent laboratory-based studies, for
28 example *Pseudoalteromonadaceae* favoring peptides, other clades behaved differently.
29 *Alteromonadaceae*, for example, grew well in the lab on many substrates but dominated in
30 seawater samples when disaccharides were added. These results highlight the diversity in DOM
31 utilization among heterotrophic bacteria and complexities in the response of natural
32 communities.

33

34 **Importance**

35 The marine DOM pool contains numerous molecular classes, which change depending on the
36 phytoplankton species, environmental conditions and interactions with other microbes, viruses
37 and predators. In turn, the availability of these macromolecular pools affects the composition and
38 function of the whole microbial community. Tracing the path between different carbon sources
39 to specific microbes is another step towards revealing the dynamic interaction between bacteria
40 and the DOM pool. This is especially important in warm and oligotrophic marine systems (e.g.,
41 Eastern Mediterranean Sea) where nutrients are scarce and may therefore affect microbial
42 activity and growth.

43

44

45 **Introduction**

46 Life depend on organic carbon, and the entire Earth system relies on the flow of carbon from
47 abiotic to biotic reservoirs, conversion into organic compounds, and subsequent remineralization
48 back to carbon dioxide (Schlesinger & Bernhardt, 2013; Summons, 1993). In the ocean, the
49 carbon cycle begins when autotrophic microorganisms convert carbon dioxide or bicarbonate
50 dissolved in seawater into organic carbon molecules. The organic carbon is then respired to meet
51 the organisms' energy needs or incorporated into biomass, mostly as macromolecular pools. In
52 phytoplankton, between ~30-65% of dry weight is composed of protein, up to 20% is nucleic
53 acids, and up to ~45% is in the form of various carbohydrates (Vargas *et al.*, 1998; Geider and
54 La Roche, 2002; Finkel *et al.*, 2016). These macromolecules are expected to be released into the
55 environment when cells die from viral lysis (Weinbauer, 2004; Kuhlisch *et al.*, 2021; Moran *et*
56 *al.*, 2022) or predation ("sloppy feeding", (Møller *et al.*, 2003; Møller, 2007)). They are also
57 released when the cells are alive, for example due to exudation of dissolved organic matter
58 (DOM) (Thornton, 2014; Lopez *et al.*, 2016; Roth-Rosenberg *et al.*, 2021), or release of vesicles
59 (Biller *et al.*, 2014).

60 Overall, the DOM pool has been estimated to contain tens of thousands of compounds (Hertkorn
61 *et al.*, 2013). Heterotrophic microbes in the ocean depend, to a large extent, on these different
62 organic compounds as a principal source of nutrients and energy (Larsson and Hagström, 1979),
63 and the composition of DOM was shown to influence microbial community function (Pinhassi *et*
64 *al.*, 2004; Gómez-Consarnau *et al.*, 2012; Becker *et al.*, 2014; Bryson *et al.*, 2017; Pontiller *et*
65 *al.*, 2020). The exact mechanisms of this relationship are not well established, but the

66 partitioning of organic carbon fractions among various heterotrophs is thought to play a
67 significant role in the resulting community structure (Sarmiento and Gasol, 2012; Bryson *et al.*,
68 2017; Pontiller *et al.*, 2020; Ferrer-González *et al.*, 2021). Heterotrophs may be specialized for
69 specific molecular classes of the DOM (herein referred to as molecular classes) pool or degrade
70 them with different efficiencies (Gómez-Consarnau *et al.*, 2012; Sarmiento *et al.*, 2016). Organic
71 molecules also serve as important signaling currencies (Keller and Surette, 2006) and changes in
72 the chemical environment alter microbial interactions (Cude *et al.*, 2012; D'Souza *et al.*, 2018;
73 Dittmar & Arnosti, 2018), adding a layer of complexity to the already complex heterotroph-
74 DOM relationship. One example is microbial cross-feeding through syntrophic interaction, that
75 can alter both DOM and microbial composition (Morris *et al.*, 2013).

76 Tracing the path of specific molecular classes between microbes would aid our understanding of
77 community function, but efforts in this area are hindered by the incredible complexity of marine
78 organic matter (Moran *et al.*, 2016; Kharbush *et al.*, 2020). Previous studies analyzing organic
79 matter degradation in environmental samples have either utilized algal exudates (e.g. (Sarmiento
80 and Gasol, 2012; Sarmiento *et al.*, 2016; Eigemann *et al.*, 2022)), or used specific molecular
81 classes such as amino acids (Keil and Kirchman, 1991; Middelboe *et al.*, 1995; Church *et al.*,
82 2000; Mary *et al.*, 2008; Zubkov *et al.*, 2008), DMSP (Ruiz-González *et al.*, 2012), glucose
83 (Rich *et al.*, 1996; Church *et al.*, 2000; Eilers *et al.*, 2000; Kirchman *et al.*, 2000; Haider *et al.*,
84 2023), pyruvate and acetate (Baltar *et al.*, 2016), and phosphonates (Dyhrman *et al.*, 2006;
85 Feingersch *et al.*, 2012; Sosa *et al.*, 2019). Several studies also compared the effect of adding
86 multiple molecular classes to natural communities, revealing differential assimilation of
87 substrates between taxa (Bryson *et al.*, 2017), and substantial transcriptional responses, which
88 differed between molecular classes along with taxon-specific responses (Pontiller *et al.*, 2020).

89 Thus, despite significant work on the role of the specific molecules mentioned above, much less
90 is known about other, broadly defined, molecular classes such as different types of
91 carbohydrates, peptides etc. This is important, as the dynamics of heterotrophic bacteria are often
92 expected to be controlled by the availability of these pools (Teeling *et al.*, 2012).

93 Here, we examine if and how natural microbial communities from the ultra-oligotrophic Eastern
94 Mediterranean Sea (EMS) respond to addition of different molecular classes: peptides, amino
95 acids, amino sugars, disaccharides, monosaccharides, and organic acids. To this end, we
96 characterized changes in community composition (16S rRNA expression) and activity (different
97 enzymatic assays) in response to amendments of different molecular classes. We also compared
98 our results with a recent study that has shown that marine heterotrophic bacteria from a diverse
99 collection, grown in lab batch culture, respond in different ways to the same molecular classes
100 (Forchielli *et al.*, 2022). While these responses could be broadly clustered by taxonomy, the
101 molecular classes ‘preferences’ were more related to the presence of specific metabolic pathways
102 (Forchielli *et al.*, 2022). This allowed us to ask whether similar preferential utilization of
103 molecular classes could be observed in a system that captures the diversity and complexity of
104 natural microbial ecosystem.

105

106 **Materials & Methods**

107 *Overview and experimental design*

108 Surface seawater (from 10m depth) were collected at the continental slope of the EMS, where the
109 bottom depth was ~800m (Latitude = 32 30.26 N; Longitude = 034 37.52 E) during November
110 11, 2019. Seawater were amended in the lab, approximately ~15 hours after collected onboard.

111 Seawater were amended with six defined molecular classes of DOM (Table 1), each at a
112 concentration of 25 μM (media composition and actual concentrations added to the bottles are
113 listed in Supplementary Table 2). In addition, inorganic nutrients were also added to make sure
114 that the heterotrophic bacteria were not N or P limited and could thus utilize the organic
115 molecular classes as carbon sources. Thus, $\sim 130 \mu\text{M}$ of NH_4 and 5 μM of PO_4 were added,
116 resulting in N:P ratio of $\sim 27:1$, in accordance with the seep water masses of the EMS (Ben Ezra
117 *et al.*, 2021) (Table 1). Seawater were incubated in quadruplicate in 4.5L bottles in running
118 seawater pools to maintain ambient temperature of $\sim 25^\circ\text{C}$ in the dark for 24 hours. Samples were
119 taken at both T_0 and T_{24} from each incubation bottle for: microbial cell abundance using flow
120 cytometry, bacterial productivity using radio labeled leucine, glucose and ATP uptake using
121 radioisotopes, and alkaline phosphatase activity (for discussion on the differences between T_0
122 and T_{24} see supplementary text 1). In addition, RNA samples for 16S amplicon sequencing were
123 taken at T_{24} .

124 **Table 1.** Summary of the different experimental treatments, including net added concentrations
125 and elemental ratios, performed on Nov. 2019 at the surface water of the EMS.

	C [μ M]	NH ₄ [μ M]	PO ₄ [μ M]	C:N	C:P	N:P
Control	0	0	0	---	---	---
Inorganic N+P	0	133	5	---	---	27
Peptides	25	133	5	0.19	5	27
Amino Acids	25	141	5	0.18	5	28
Disaccharides	25	133	5	0.19	5	27
Monosaccharides	25	133	5	0.19	5	27
Amino sugars	25	137	5	0.18	5	27
Organic Acids	25	133	5	0.19	5	27

126

127 *Bacterial productivity*

128 Bacterial productivity (BP) was estimated using the ³H-leucine incorporation method (Simon and
129 Azam, 1989) and is described in detailed by (Reich *et al.*, 2022). Triplicate 1.7ml of seawater
130 were incubated with ³H-leucine (20 nmol leucine L⁻¹) for 4h at ambient temperature of ~25°C in
131 the dark immediately after sampling. The incorporation was terminated by adding 100 μ l of cold
132 trichloroacetic acid (TCA). Killed blanks containing seawater, the radiolabeled leucine and TCA
133 added immediately upon collection (no incubation) were also undertaken and subtracted from the
134 sample reads. The samples processed using the micro-centrifugation protocol (Simon and Azam,
135 1989). Scintillation cocktail with high affinity to beta radiation (ULTIMA-GOLD) was added
136 before counted using TRI-CARB 2100 TR (PACKARD) scintillation counter.

137 *Glucose and ATP bulk uptake*

138 Bulk uptake rates of Adenosine 5'-triphosphate and Glucose D[-³H(N)] were estimated using
139 modified assay adapted from (Alonso-Sáez *et al.*, 2012). Triplicate 20 ml of seawater were
140 spiked immediately after sampling with either ³H-Adenosine Triphosphate or ³H-D-Glucose
141 (added concentration of 0.2 nM for each substrate, 0.1548 μ Ci and 0.1836 μ Ci in sample

142 respectively) and incubated for 4h at ambient temperature in the dark. The incorporation was
143 terminated by filtration of the samples onto 0.22 µm polycarbonate filters followed by
144 subsequent rinsing with 5 ml of 0.22 µm filtered seawater. Killed blanks containing seawater, the
145 radiolabeled substrate and formaldehyde (2% final concentration) added immediately upon
146 collection and 15 minutes prior to the spike were also undertaken and subtracted from the sample
147 reads. A scintillation cocktail with high affinity to beta radiation (ULTIMA-GOLD) was added
148 before counted using TRI-CARB 2100 TR (PACKARD) scintillation counter.

149 *Alkaline phosphatase activity (APA)*

150 APA was determined by the 4-methylumbelliferyl phosphate (MUF-P: Sigma M8168) method
151 (Thingstad and Mantoura, 2005). After the addition of substrate to a final concentration of 50
152 µM, samples were incubated in the dark at ambient temperature for 3/4 hour.

153 *RNA extraction, DNA digestion, cDNA synthesis*

154 Bacterial community/activity was assessed by 16S rRNA. Approximately ~4.4 L of SW from
155 each incubation bottle was filtered directly onto 0.2 µm filters, added with RNAsave and stored
156 in -80°C until extraction. RNA was extracted using RNeasy® PowerWater® Kit following the
157 manufacture protocol, including DNase treatment. RNA was transcribed into cDNA using iScript
158 cDNA Synthesis.

159 *16S rRNA sequencing*

160 Sequencing was performed using primers 515F and 926R (Walters *et al.*, 2015). Amplicons were
161 generated using a two-stage polymerase chain reaction (PCR) amplification protocol. First stage
162 PCR amplification was carried out in 25 µl reactions using MyTaq Red Mix (BIO-25044,
163 Meridian Bioscience). The amplification parameters were set as follows: 95° C for 5 min,

164 followed by 28 cycles at 95°C for 30s, 50°C for 30s, and 72°C for 1 min. A final, 5-min
165 elongation step was performed at 72°C. Products were verified on a 1% agarose gel before
166 moving forward to the 2nd stage. One microliter of PCR product from the first stage
167 amplification was used as template for the 2nd stage, without cleanup. Cycling conditions were
168 98°C for 2 minutes, followed by 8 cycles of 98°C for 10s, 60°C for 1min and 68°C for 1min.
169 Libraries were then pooled and sequenced with a 15% phiX spike-in on an Illumina MiSeq
170 sequencer employing V3 chemistry (2x300 base paired-end reads). Library preparation and
171 sequencing were performed at the Genomics and Microbiome Core Facility (GMCF; Rush
172 University, IL, USA).

173 *16S rRNA sequence analysis*

174 All sequences were analyzed using Dada2 pipeline (Callahan *et al.*, 2016) and the software
175 packages R (R Development Core Team, 2011) and Rstudio (R Team, 2020). Forward and
176 backward primers were trimmed, forward and backward reads truncated after quality inspections
177 to 250 and 230 bases respectively. After sequences merging, a consensus length only between
178 400 and 430 bases was accepted. Finally, ASVs that have less than 100 in total (all samples)
179 were removed. Silva database version 138 (Quast *et al.*, 2012) was used for taxonomic
180 assignment. All chloroplasts, mitochondria, archaea, eukaryotes and Amplicon sequence variants
181 (ASVs) without any taxonomic affiliation were discarded from downstream analyses.

182 *Statistics*

183 Data pre-processing and statistical analyses were performed using the R statistical programming
184 language (R Development Core Team, 2011; R Team, 2020). One-way ANOVA and post-hoc
185 Tukey test were performed to compare between the treatments on each time points separately
186 (Figures 2 and 3, Supplementary Table 1) using multcompView (Graves *et al.*, 2019) and dplyr

187 (Wickham et al., 2023) packages. Paired t-test with Bonferroni correction was used to compare
188 the means between time points of each treatment (Supplementary Figures 3 and 4) using the
189 packages tidyverse (v1.3.0; (Wickham et al., 2019), rstatix (Kassambara, 2023b) and ggpubr
190 (Kassambara, 2023a). PERMANOVA test was used to test the significance of the NMDS plots
191 distribution (Figure 4). Mantel test with 9999 permutations examining the Spearman's
192 correlation was used to test the correlation between the BioCyc and 16S results (Figure 6) using
193 vegan package (Oksanen et al., 2022). Plots were originated using ggplot2 package (Wickham,
194 2016).

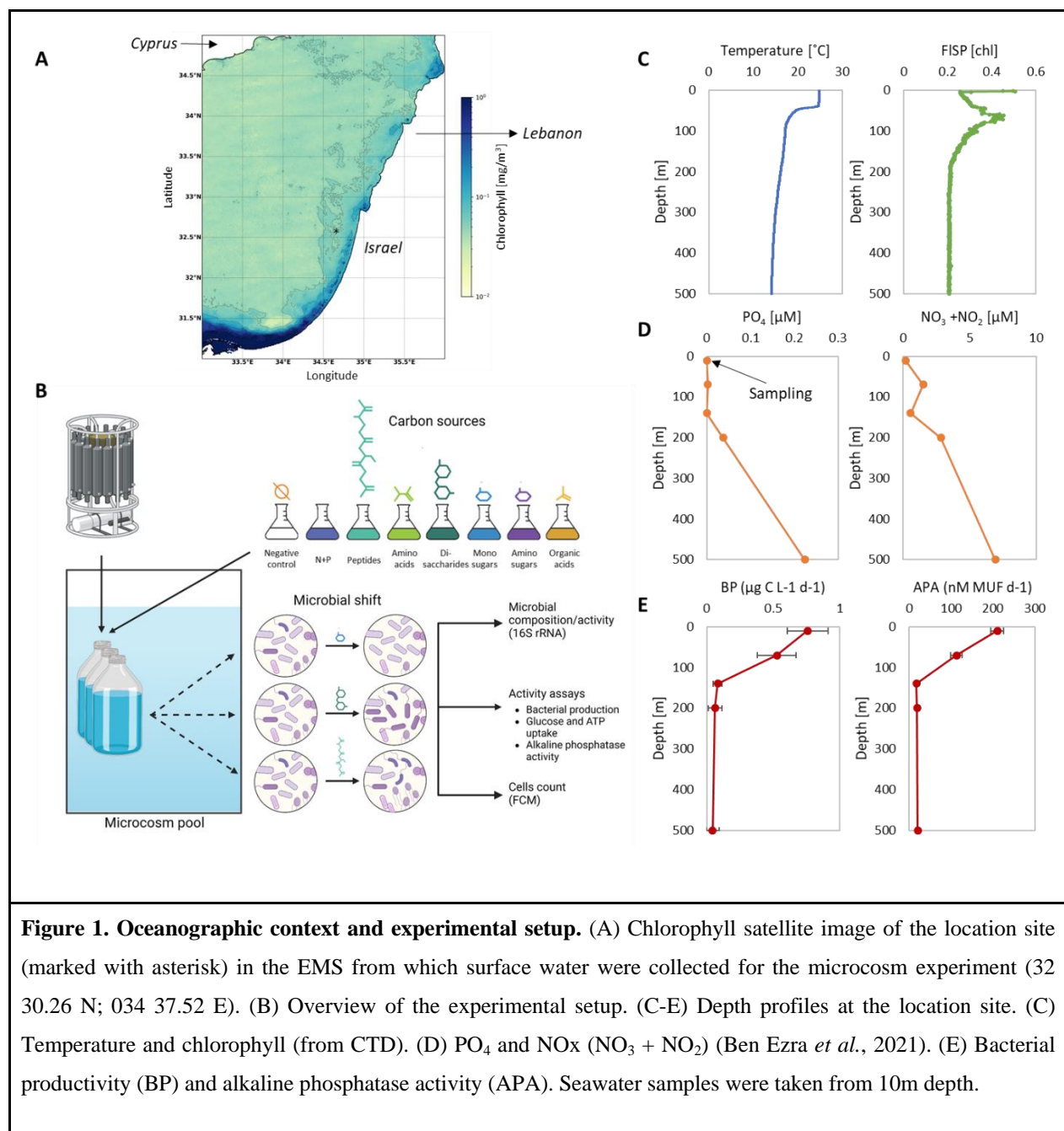
195

196 **Results**

197 *Initial seawater characteristics and experimental setup*

198 The marine microbial community to which we added different molecular classes was from a
199 transition region between coastal and open-ocean, oligotrophic waters in the EMS (Figure 1A).
200 The experiment was performed using surface water (10m depth) collected from an offshore
201 location (~800m water depth). Water was collected at the end of fall, moving into winter, after
202 11-12 days of constant Easterly or Southerly winds and no rain. The vertical temperature profile
203 indicates that the water column was still stratified, with ~25°C in the upper 50m (Figure 1C) and
204 salinity of ~39.5 ppt throughout (Supplementary Figure 1B). Orthophosphate in the surface water
205 was below the limit of detection (Figure 1D), and alkaline phosphatase activity (APA) was
206 relatively high, suggesting phosphorus-limitation for microbes (Figure 1E). Surface NO₃ + NO₂
207 concentration was 0.19µM (Figure 1D), and surface primary productivity values were 0.35±0.03
208 µg C L⁻¹ h⁻¹ (Supplementary Figure 2E), both of which were somewhat higher than previously

209 reported for a parallel season in the open-ocean Eastern Mediterranean (Ben Ezra *et al.*, 2021;
210 Reich *et al.*, 2022). This suggests that despite the stratification, winter mixing had begun, in
211 agreement with results from a time-series study from a nearby location (Ben Ezra *et al.*, 2021).
212 To characterize the response of this natural community to different classes of labile DOM, we
213 amended the collected seawater with six different molecular classes: peptides, amino acids,
214 monosaccharides, disaccharides, amino sugars and organic acids, each at 25 μ M (see
215 Supplementary Table 2 for detailed media composition, which mirrored those of a previous in
216 vitro experiment (Forchielli *et al.*, 2022)). We also included a negative control without any
217 modification, and a control amended only with NH₄ and PO₄, which were added to mitigate any
218 potential inorganic nutrient limitation (Figure 1B, Table 1).



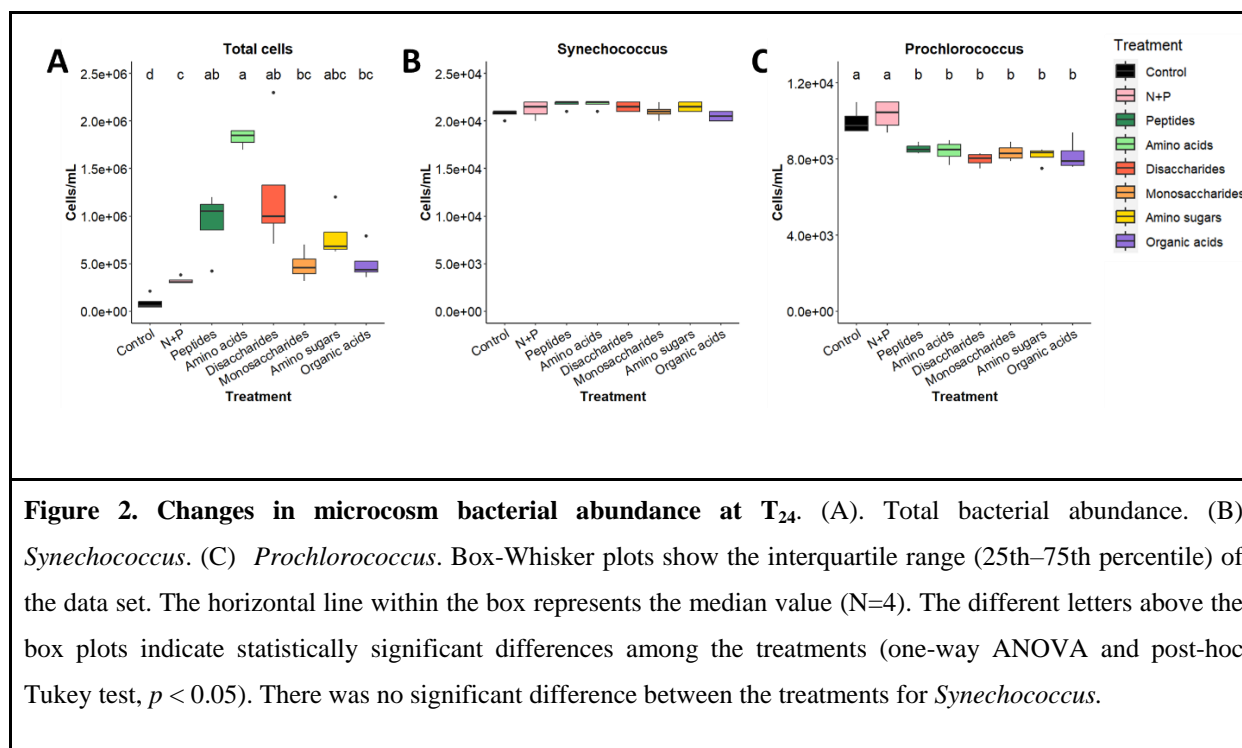
219

220 *Microbial Abundance*

221 After 24 hours incubation, total bacterial abundance was $\sim 5 \times 10^4$ cells ml⁻¹ in the un-amended
 222 controls, and significantly increased (~ 3.5 fold) in the N+P addition (Figure 2A). Peptides,
 223 amino acids and disaccharides all elicited an additional ~ 3 -5.5 fold increase above the N+P

224 treatment bottles (P -value <0.05 , one-way ANOVA), whereas monosaccharides, amino sugars
225 and organic acids elicited smaller increases which were not statistically significant.

226 Two autotrophic prokaryotes groups were identified: *Synechococcus* ranging from 2 - 2.5×10^5
227 cells ml^{-1} (Figure 2B) and *Prochlorococcus* ranging from 7.5×10^3 - 1.3×10^4 cells ml^{-1} (Figure
228 2C). The addition of molecular classes reduced *Prochlorococcus* (but not *Synechococcus*) counts
229 relative to the un-amended and N+P controls (Figures 2B and C).



230

231 *Bacterial activity assays*

232 BP, a commonly used general measure of heterotrophic bacterial activity, is measured by the
233 incorporation of radiolabeled leucine, and thus represents the uptake of amino acids and their
234 incorporation into biomass. After 24 hours bulk BP significantly increased for all molecular
235 classes compared to both the un-amended and N+P controls (Figure 3A), with the largest

236 increase observed with amino acids, as previously shown (Middelboe *et al.*, 1995; Zubkov *et al.*,
237 2008). In contrast to the bulk BP, BP/cell increased significantly in relation to the un-amended
238 and N+P controls only after the addition of amino acids (Figure 3B).

239 As opposed to bacterial productivity, bulk uptake rate of glucose and ATP either decreased or
240 did not change relative to the control and N+P (Figure 3 C, E), and the per-cell values
241 significantly decreased (Figure 3 D, F). Notably, already at T₀ (right after the addition of the
242 macromolecular classes) glucose uptake rates for monosaccharides, disaccharides and amino
243 sugars were significantly lower compared with the other treatments (*P*-value<0.05, one-way
244 ANOVA, supplementary Table 1, Supplementary Figure 4C). Since glucose was one of the
245 monosaccharides used for these experiments, it is possible that the decrease in the uptake of the
246 radiolabeled sugar is due to competition between the “hot” (radiolabeled) and “cold” substrate.
247 However, the decrease in disaccharides and amino sugars is less expected and may be due to
248 cross-reactivity of the transporters or to catabolite repression, as discussed in more detail in
249 supplementary text 2.

250 In addition to measuring the uptake rates of amino acids, glucose and ATP, we also measured
251 extracellular alkaline phosphatase activity (APA). Higher AP activity is expected when PO₄
252 concentration are low (Cembella *et al.*, 1982), and thus a good estimator for phosphorous
253 starvation. Initial APA values were similar across all treatments, but lower than measured *in-situ*
254 at the sampling site (~60 compared to ~240 nM MUF/day in the surface water, compare Figure
255 3G and Figure 1E). Bulk APA significantly increased compared to the un-amended and N+P
256 controls only for amino acids, but some degree of increase was also observed for most other
257 treatments (Figure 3G), possibly as a result of the increased bacterial abundance. In contrast,

258 APA/cell significantly decreased in all treatments compared to the control, which is expected
259 since phosphate was added (Figure 3H).

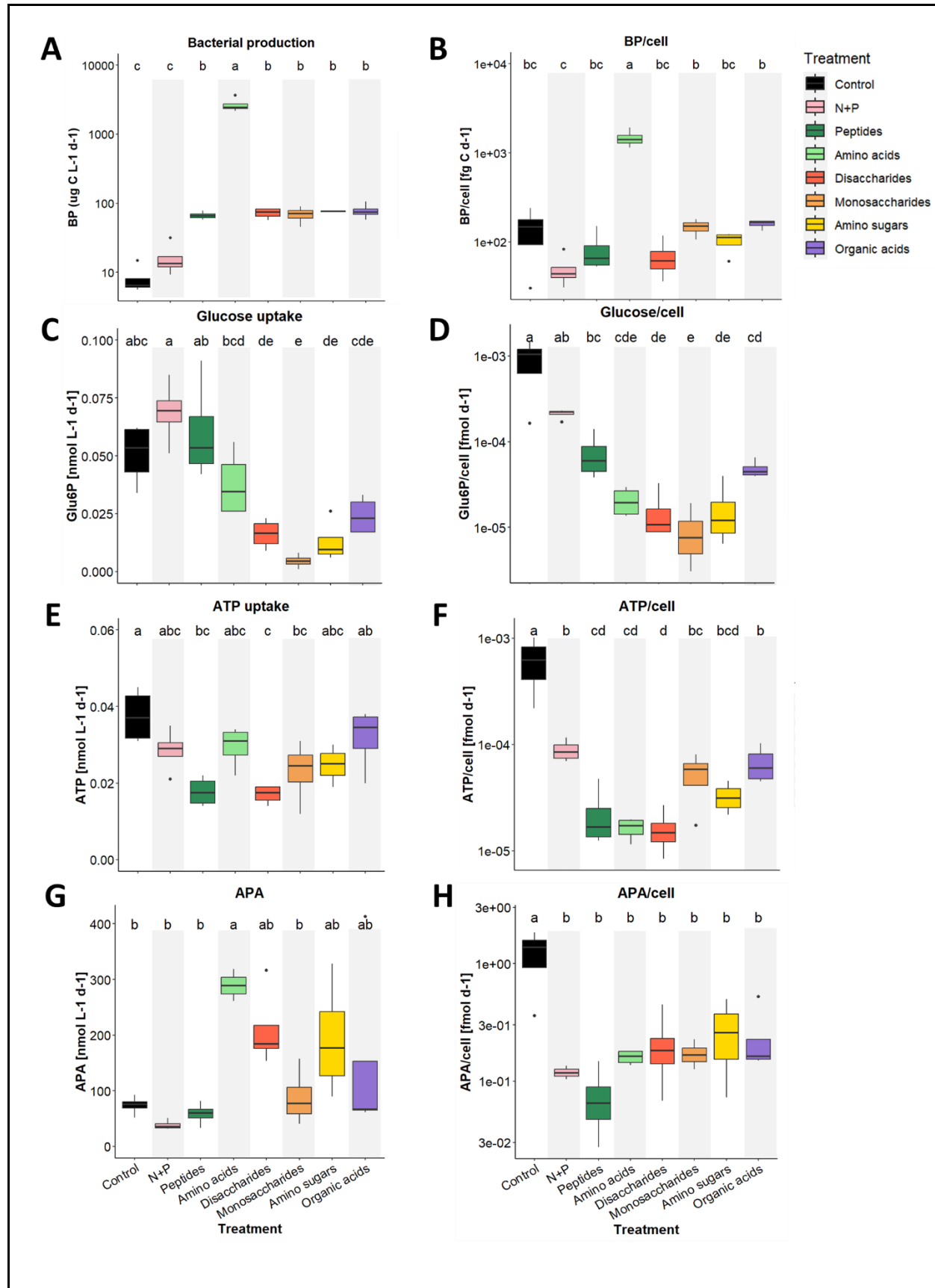


Figure 3. Different parameters of bacterial activity as bulk and per-cell at T₂₄. (A, B) Bacterial production. (C, D) Glucose uptake. (E, F) ATP uptake. (G, H) Alkaline phosphatase activity (APA). Note the logarithmic Y-axis on A and on the right panel. Box-Whisker plots show the interquartile range (25th–75th percentile) of the data set. The horizontal line within the box represents the median value (N=4). The different letters above the box plots indicate statistically significant differences among the treatments (one-way ANOVA and post-hoc Tukey test, $p < 0.05$). Bulk and per-cell BP uptake rates with amino acids were corrected to consider the “cold” Leucin concentration (1.9 μM , see supplementary text 2).

260

261 *Changes in microbial community composition*

262 To determine whether the microbial community composition was altered in response to the
263 different added molecular classes, we amplified and sequenced the 16S rRNA (i.e. from
264 extracted total RNA). Observed changes are therefore due to both changes in ribosomal RNA
265 gene expression (associated with increases in activity or growth rate) and changes in cell
266 numbers (Salazar *et al.*, 2019). The un-amended and N+P controls samples grouped together and
267 close to the surface (10m) and half-DCM (70m) samples collected in the field (Figure 4A). The
268 field, control and N+P samples were also more diverse than the samples to which molecular
269 classes were added (alpha diversity, Supplementary Figure 5), and dominated by cyanobacteria
270 (mostly *Synechococcus* but also *Prochlorococcus*) and alphaproteobacteria (SAR11, SAR 116 or
271 AEGEAN-169) (Figure 4C). The 10m sample, from which water were taken for the experiment,
272 was composed of ~45% cyanobacteria, ~10% SAR202 and ~8% SAR11 (clade 1), with other
273 families below 5%. In addition to cyanobacteria and alphaproteobacteria, the un-amended and
274 N+P controls also had more Flavobacteria (~6%) and few gammaproteobacteria families:
275 *Vibrionaceae* (~5-15%), and (for the N+P control) KI89A and SAR86 clades (~5-15%).
276 The addition of each molecular class elicited a different change in the microbial community
277 rRNA profile, and in many of these cases it resulted in the growth of a different clade of

278 heterotrophic bacteria (Figure 4 B, C). The peptide treatment, which was dominated by
279 *Pseudoalteromonadaceae*, clearly differed from all others in the NMDS ordination. Two other
280 treatments, disaccharides and amino sugars also each group separately. The disaccharide
281 treatments were dominated by *Alteromonadaceae*, *Pseudoalteromonadaceae* and to some extent
282 *Vibrionaceae*, while the amino sugars treatment was dominated by *Vibrionaceae*. The
283 community growing on organic acids was also dominated by *Vibrionaceae* but also by
284 *Marinomonadaceae*, which were also quite abundant in the amino acids and most
285 monosaccharides treatments. Overall, in terms of relative abundance, the dominant family in all
286 treatment except peptides was *Vibrionaceae*, with the highest percentages observed for amino
287 acids and amino sugars (~75%), followed by monosaccharides, disaccharides and organic acids
288 (~25-50%) (Figure 4C).

289 Within some of the families there were also higher-resolution patterns in the relative abundance
290 of specific Amplicon Sequence Variants (ASVs). The most abundant family, *Vibrionaceae*, was
291 comprised of ~6-8 prevalent ASVs, three of which were specific for *Photobacterium sp.* (a
292 common fish pathogen), and the others could not be identified to a higher resolution than the
293 family level. The *Photobacterium* ASVs were relatively abundant only in response to amino
294 sugars, and actually decreased in relative abundance in other treatments, whereas the other ASVs
295 were unspecific and found among all treatments without any clear patterns (Supplementary
296 Figures 6, 7A). In contrast, *Pseudoalteromonadaceae* had 3 main ASVs with ~90-97% identity.
297 The first and unspecific ASV, ASV3, was very dominant for peptides while the other two, one of
298 which matches the genus *Psychrosphaera*, were mostly found in two of the disaccharide's
299 treatment (Supplementary Figure 7B). In contrast, no clear intra-family patterns were observed
300 for *Alteromonadaceae* and *Marinomonadaceae* (Supplementary Figure 7C, D). ASV belonging

301 to the four most abundant families responding to the molecular classes were not identified in the
302 original seawater (from 10m depth), except for one ASV of *Pseudoalteromonadacea* with
303 relative abundance of 0.03%.

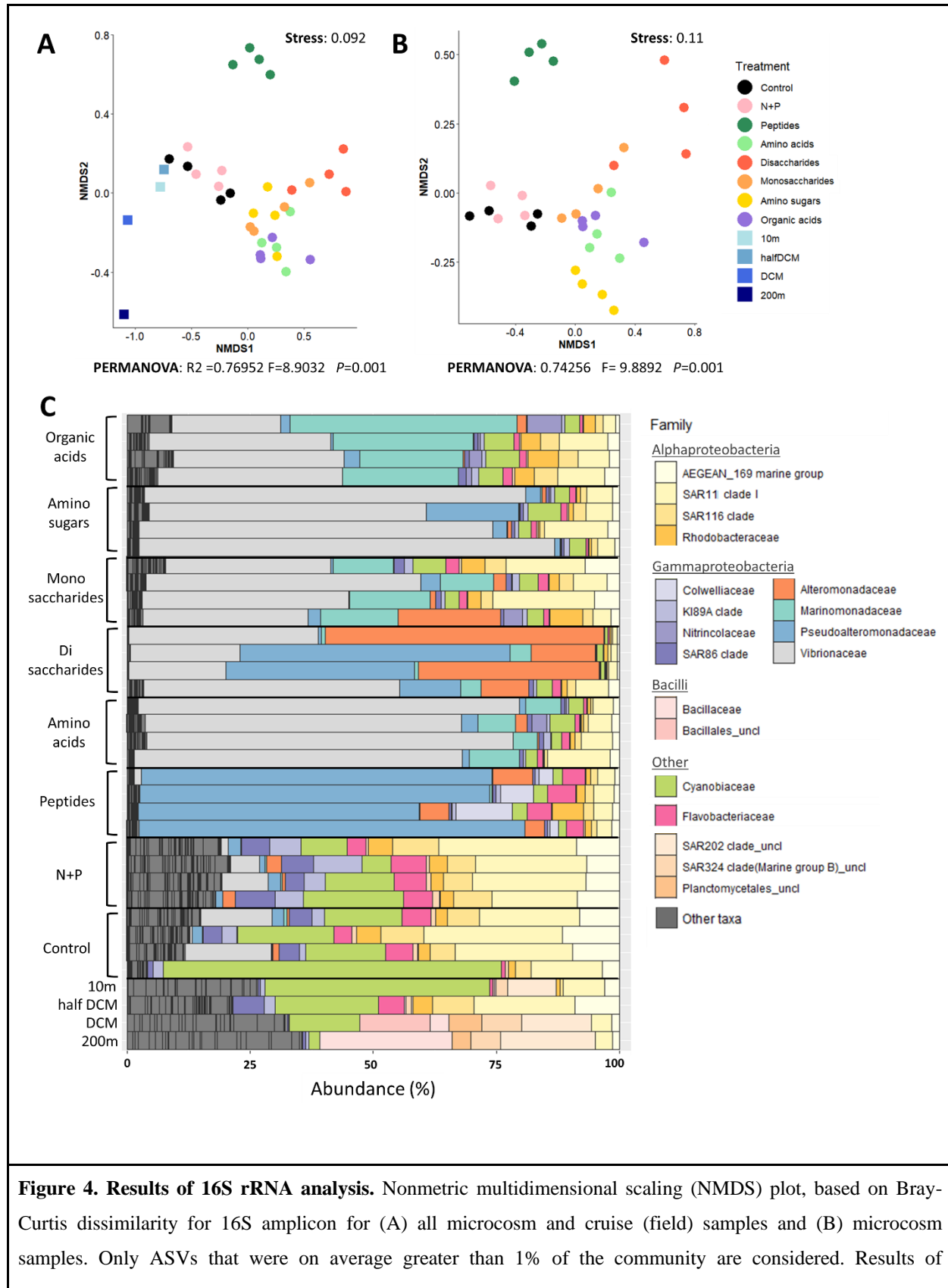


Figure 4. Results of 16S rRNA analysis. Nonmetric multidimensional scaling (NMDS) plot, based on Bray-Curtis dissimilarity for 16S amplicon for (A) all microcosm and cruise (field) samples and (B) microcosm samples. Only ASVs that were on average greater than 1% of the community are considered. Results of

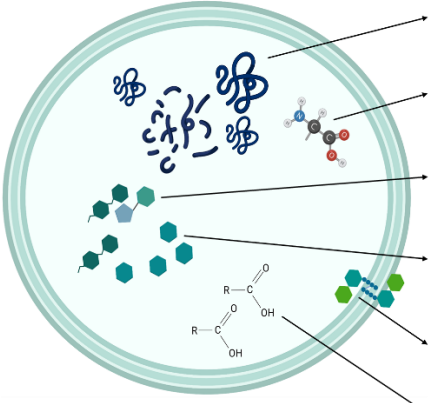
PERMANOVA test are shown in both panels. (C) Stacked bar chart showing relative proportions (percentages of 16S rRNA sequences) of microbial community at T24 at the family level. *Pseudoalteromonadaceae* responded primarily to peptides, and (with *Alteromonadaceae*) to disaccharides; *Marinomonadaceae* responded to organic acids, and *Vibrionaceae* to everything but peptides. Uncl=uncultured. Other taxa=families not greater than 5% in any sample.

304

305 ***Differences between patterns of carbon source utilization in laboratory cultures and in natural***
306 ***communities.***

307 How do the results presented above compare with a set of laboratory experiments in which 63
308 selected strains of marine heterotrophic bacteria were grown with the same molecular classes
309 (Forchielli et al., 2022)? As shown in Figure 5, the change in relative abundance of some specific
310 families in our microcosm experiment was consistent with the growth of their cultured
311 representatives in lab cultures. For example, *Pseudoalteromonadaceae*, the dominant family
312 observed when peptides were added to natural seawater, also grew well on peptides in
313 monocultures (Figure 5). *Pseudoalteromonadaceae* were also very dominant in two
314 disaccharides samples in the microcosm, yet only one cultured strain, *Pseudoalteromonas citrea*,
315 was able to grow on disaccharides (Forchielli et al., 2022), suggesting the potential for intra-
316 family diversity in the ability to utilize this molecular class. *Rhodobacteraceae*, although not one
317 of the most common families, also behaved similarly, growing well in lab monocultures on
318 organic acids and monosaccharides and in most microcosm replicates where organic acids and
319 monosaccharides were added (~2-5%, compared to <2% in the other treatments). The growth of
320 other clades, however, was less consistent between the laboratory cultures and natural
321 communities in the microcosm. Lab cultures of *Alteromonadaceae*, for example, grew well on
322 amino acids, disaccharides and amino sugars, whereas they dominated in the microcosms only

323 when disaccharides were added. In addition, *Vibrionaceae*, which were common in all
 324 microcosm treatments except peptides, grew in lab cultures mostly on amino acids and peptides
 325 (Figure 5, (Forchielli et al., 2022)).



	Laboratory cultures (OD)			Microcosm – log2 fold change			
Peptides	<i>Pseudoalt.</i> (0.69±0.28) N=3/3	<i>Alteromonas</i> (0.6±0.3) N=6/6	<i>Vibrio</i> (0.51±0.29) N=3/3	<i>Pseudoalt.</i> (5.2±0.2)			
Amino acids	<i>Vibrio</i> (0.48±0.02) N=3/3	<i>Pseudoalt.</i> (0.44±0.14) N=3/3	<i>Alteromonas</i> (0.41±0.09) N=5/6	<i>Marinomonas</i> (5.2±0.4)	<i>Vibrio</i> (4.1±0.1)		
Disaccharides	<i>Alteromonas</i> (0.46±0.12) N=6/6	<i>Rhodobacter</i> (0.54±0.18) N=5/7		<i>Alteromonas</i> (3.9±1.2)	<i>Marinomonas</i> (3.2±1.4)	<i>Vibrio</i> (2.9±0.7)	<i>Pseudoalt.</i> (2.7±2.9)
Mono-saccharides	<i>Rhodobacter</i> (0.28±0.12) N=5/7*			<i>Marinomonas</i> (6.1±0.3)	<i>Vibrio</i> (3.3±0.4)		
Amino sugars	<i>Alteromonas</i> (0.68±0.27) N=3/6			<i>Vibrio</i> (4.2±0.3)			
Organic acids	<i>Rhodobacter</i> (0.46±0.1) N=7/7			<i>Marinomonas</i> (7.2±0.5)	<i>Vibrio</i> (3±0.4)		

Figure 5. Bacterial growth on phytoplankton-derived molecular classes in lab (monoculture) and in the microcosm (mixed community). Proteins, including **peptides** and **amino acids**, are key components in the cell and comprise up to 60% of its dry weight (Geider and La Roche, 2002). **Sugars** are energy sources, comprising in our experiments **disaccharides** and **monosaccharides**, as well as **amino sugars** such as N-acetylglucosamine (GlcNAc) which are major components of the cell wall (Konopka, 2012). **Organic acids** are common metabolites produced and consumed by different microorganisms, and genes for their utilization were shown to be upregulated in bacterioplankton following phytoplankton bloom (Rinta-Kanto *et al.*, 2012). Colors in the table represent different families. For the microcosm, only families with an average (N=4) log2 fold change>1.5 are shown. In the lab, we include only genera with a minimum of 3 strains tested, and which were able to grow above average OD_{600nm} of 0.4 (Forchielli et al., 2022). N represents the number of strains able to grow on each molecular class. **Rhodobacter* was the only genus to show any substantial growth on monosaccharides, and thus included in the table although its average OD was lower than 0.4.

326

327 Is there a correlation between the number of metabolic pathways for the degradation of each
 328 carbon source type, encoded in the genome of each heterotrophic clade, and its propensity to
 329 become dominant in response to this carbon source? As shown in Figure 6, there was no

330 statistically significant correlation between the relative increase in rRNA transcripts for each
331 clade in response to the different molecular classes and the average number of pathways for the
332 degradation of these molecular classes. However, disaccharides and amino sugars did show a
333 trend for positive correlation (Figure 6D, E and supplementary text 3).

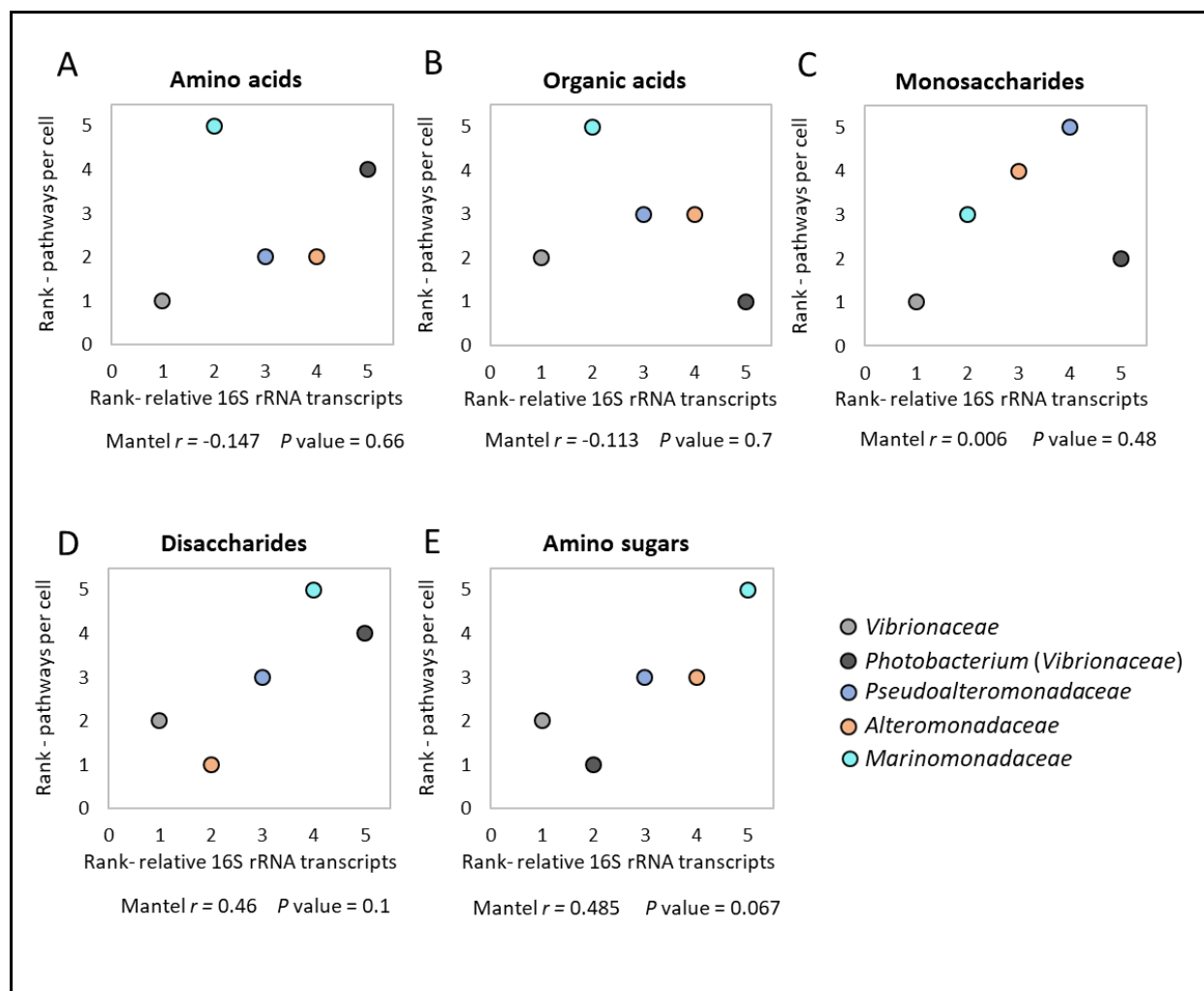


Figure 6. Correlation between metabolic pathways (BioCyc) and average relative abundance/activity (16S rRNA transcript amplicons) for the five most abundant families. (A) Amino acids. (B) Organic acids. (C) Monosaccharides. (D) Amino sugars (E) Disaccharides. Data shown are ranked values based on Supplementary Tables 4 and 5 and is further discussed in supplementary text 3. r and P -values are the results of Mantel test with 9999 permutations examining the Spearman's correlation. Black lines are linear trendlines.

334

335 **Discussion**

336 The goal of this study was to ask how a natural marine microbial community from oligotrophic
337 waters responds to different molecular classes (peptides, amino acids, disaccharides,
338 monosaccharides, amino sugars and organic acids) in terms of activity and community
339 composition. We identified four main Gammaproteobacteria families (*Vibrionaceae*,
340 *Pseudoalteromonadaceae*, *Alteromonadaceae* and *Marinomonadaceae*) that responded
341 specifically to the addition of different molecular classes. Below we discuss these results in light
342 of other studies asking how different types of organic matter affect marine microbial
343 communities or individual bacterial strains, using them to illuminate how specific metabolic
344 pathways, metabolic regulation and microbial interactions may all play a role in determining
345 community dynamics.

346

347 *The addition of distinct molecular classes of DOM induces the growth of relatively rare but*
348 *ecologically relevant heterotrophic families.*

349 The four main Gammaproteobacterial families which responded to the addition of the molecular
350 classes are mostly rare in the original seawater community, which was dominated by alpha-
351 proteobacteria and cyanobacteria, as previously observed (Haber et al., 2022; Roth Rosenberg et
352 al., 2021). Yet these clades are sometimes relatively abundant in specific oceanic niches such as
353 marine particles (Haber et al., 2022; Lyons et al., 2007; Roth Rosenberg et al., 2021; Takemura
354 et al., 2014). They also tend to become dominant during mesocosm experiments in response to
355 additions of both specific molecules such as glucose (Eilers *et al.*, 2000; Haider *et al.*, 2023) and
356 complex mixtures (e.g. high molecular weight DOM, (Sosa *et al.*, 2015), and see below).

357 Previous studies have shown that rare microorganisms have higher respiration rates compared to
358 more abundant bacteria, suggesting that despite their overall rarity these copiotrophic bacteria
359 have an important role in the remineralization of organic carbon (Munson-McGee *et al.*, 2022).

360 Several previous studies have compared the responses of natural communities to the addition of
361 different molecular classes, in relatively productive coastal or brackish locations (the California
362 coast (Bryson *et al.*, 2017), and the Baltic Sea (Pontiller *et al.*, 2020). Similar to our study,
363 different molecular classes elicited different community responses in terms of relative abundance
364 and subsequent substrate uptake. For example, *Alteromonadaceae* responded both to
365 polysaccharides in the California coast (Pontiller *et al.*, 2020) and to disaccharides in our study.
366 Yet in many cases the specific clades responding were different. For example, *Flavobacteria*
367 from the California coast responded primarily to glucose and starch, and from the Baltic Sea to
368 proteins, yet this clade was not one of the main responders in our study. It did, however, grow in
369 the un-amended control, N+P and peptides treatment but decreased in relative abundance in the
370 other treatments. Conversely, *Vibrionaceae*, which were the main responders to almost all
371 molecular classes in our study, did not respond in either of the other ones. However, in another
372 study conducted with water from the mesopelagic North Atlantic, addition of the organic acids
373 pyruvate and acetate induced, among other, the growth of *Vibrionaceae*, as in our study (Baltar
374 *et al.*, 2016). Thus, further studies are needed in order to determine whether these differences are
375 due to technical aspects (e.g. amount of organic matter added or incubation time), or to
376 ecological factors such as the trophic state of the ecosystem (oligotrophic marine waters vs
377 productive coastal and brackish) or the season sampled.

378 The molecular classes we chose represent a significant part of the biomass of phytoplankton,
379 which would be released as phytoplankton die, e.g. during the late stages of a bloom. Indeed,

380 phytoplankton blooms are often followed by a succession of heterotrophic bacteria, especially of
381 *Roseobacters*, *Flavobacteria* and members of the Gammaproteobacteria such as
382 *Alteromonadaceae* (Riemann *et al.*, 2000; Fandino *et al.*, 2001; Pinhassi *et al.*, 2004; Buchan *et*
383 *al.*, 2014). For example, natural macroalgae blooms were shown to induce the growth of
384 *Vibrionaceae*, possibly related to their ability to degrade brown algal polysaccharides (Takemura
385 *et al.*, 2014; Martin-Platero *et al.*, 2018). In several occasions, *Vibrionaceae* were shown to
386 comprise up to ~50% of total microbial community (fraction of 16S amplicons, (Zhang *et al.*,
387 2018)). *Prochlorococcus* exudates, on the other hand, dramatically induced the growth of
388 *Pseudoalteromonadaceae* in open ocean water from the EMS (Eigemann *et al.*, 2022), and based
389 on the results presented here we speculate that this might be due to these exudates being protein-
390 or disaccharide-rich (Figure 4). It is noteworthy also that amino acids, peptides and
391 disaccharides induced the highest increase in cell abundance, suggesting that these molecular
392 classes can be used to form biomass, while others can lead mainly to respiration. This could also
393 affect the perceived changes in community composition.

394

395 *Relationship between specific metabolic pathways and microbial growth on each carbon source*
396 *type.*

397 Bacterial growth depends primarily on the ability to utilize the specific nutrient sources present.
398 We have previously shown that such metabolic preferences can be captured by the relative
399 abundance of some metabolic pathways or a handful of key enzymes (Forchielli *et al.*, 2022). For
400 example, in the lab, growth on disaccharides, monosaccharides and acidic sugars was associated
401 with an enrichment in carbohydrate metabolism pathways (e.g. galactose, starch and sucrose)
402 and depleted in pathways for amino acid utilization. In the complex community studied here, we

403 observed a positive (yet not significant) correlation between the genetic capacity for degrading
404 disaccharides and amino sugars and the dominance of specific clades when these molecular
405 classes were added (Figures 6D and E). For example, *Vibrionacea* (as well as a sub-group,
406 *Photobacterium*) ranked first in both average amino sugars pathways per genome and in relative
407 abundance after 24 hours (Figure 6E). This is supported to some extent by a study that tested the
408 uptake of the amino sugar N-acetyl-D-glucosamine (NAG) among different bacteria, where no
409 clear pattern relative to phylogeny was found, except that all 19 *Vibrionacea* took up NAG
410 (Riemann and Azam, 2002). Similarly, both *Vibrionacea* and *Alteromonadaceae* had relatively
411 more pathways for the utilization of disaccharides per cell, and indeed these two clades were the
412 dominant ones in the disaccharide-treated microcosms (Figure 6D). This is partly in accordance
413 with another incubation experiment where *Alteromonadaceae* responded to the addition of
414 polysaccharides by growing and expressing genes related to motility and glycogen utilization
415 (Pontiller *et al.*, 2020). *Alteromonadaceae* have also been suggested to degrade complex
416 carbohydrates in when incubated with natural organic material such as jellyfish detritus (Tinta *et*
417 *al.*, 2023), and several *Alteromonas* strains have been shown to degrade multiple polysaccharides
418 in the lab (e.g. (Koch *et al.*, 2019)).

419 In contrast to disaccharides and amino sugars, we did not observe any correlation between the
420 relative abundance of specific clades in response to amino acids, organic acids and
421 monosaccharides and the presence of degradation pathways for these molecular classes. When
422 individual strains were tested in the lab (Forchielli *et al.*, 2022), growth on these molecular
423 classes was not associated with the number pathways for their utilization but rather with other
424 pathways that may interact with them. For example, growth on organic acids was associated with
425 enrichment for specific portions of the ethylmalonyl-CoA pathway, which is an alternative to the

426 glyoxylate shunt used in growth on some organic acids (Forchielli et al., 2022). This would not
427 have been captured in our more simple analysis.

428 It should be noted that we did not test here for correlations between the genetic capacity to
429 degrade peptides and dominance when peptides were added, since growth on peptides depends
430 primarily on their degradation by a wide range of relatively less characterized extracellular and
431 intracellular peptidases. However, there are indications that *Pseudoalteromonas*, the dominant
432 family growing on peptides in both laboratory monocultures and our mesocosms, is an
433 important player in peptides degradation in marine environments (Zhao *et al.*, 2012; Tang *et al.*,
434 2020; Tinta *et al.*, 2023).

435

436 *Are the effects of molecular classes on enzymatic activity and cell uptake due to changes in*
437 *community structure or function?*

438 A surprising observation in our study is that, while bulk amino acid uptake (BP) increased in all
439 treatments, glucose and ATP uptake did not, and actually decreased on a per-cell basis (Figure
440 3). Similar observations were reported in seawater samples from the Gulf of Mexico, in which
441 bulk uptake rates of glucose decreased in response to high molecular weight DOM and increased
442 with the addition inorganic nutrients (Skoog *et al.*, 1999). Glucose is considered to be a common
443 organic molecule in the ocean (Rich *et al.*, 1996), and the addition of glucose can increase
444 heterotrophic microbial activity and viability in the EMS (Rahav *et al.*, 2019). The decrease in
445 glucose uptake in response to a wide range of molecular classes could, in principle, be explained
446 by a shift in community composition, to one where the dominant organisms do not utilize
447 glucose (such as some SAR11 strains, (Schwalbach *et al.*, 2010)). However, since *Vibrionacea*
448 and *Marinomonadacea* were the dominant organisms in most mesocosms, including those to

449 which monosaccharides were added, it is less likely that the decrease in glucose uptake is due to
450 the shift in community composition. We propose that the reduction in glucose uptake is more
451 likely to be explained by a change in the physiology of the dominant community members, for
452 example through catabolite repression, where the addition of one carbon source reduces the
453 expression of pathways for the use of another (e.g. downregulation of glucose transporters).

454 In contrast to glucose, which cannot be used by all marine bacteria, ATP is a key metabolite in
455 every organism, involved in thousands of metabolic reactions, and found in all cells at millimolar
456 concentrations. ATP taken up from the environment can provide the cells with both energy and
457 phosphorus, which is often limiting in the EMS (Ben Ezra *et al.*, 2021; Reich *et al.*, 2022).
458 Similar to the decreased APA activity, the decrease in ATP uptake across all experimental
459 conditions is most likely related to the alleviation of phosphate limitation by the addition of PO₄
460 (Sebastián *et al.*, 2012). This also suggests that any change in community composition likely
461 represents bacteria able to use these the added molecular classes rather than a response to
462 phosphorus starvation.

463 As opposed to glucose and ATP, the per-cell uptake rates of leucine (the amino acid used for the
464 BP assay) remained stable after 24 hours, with the exception of the amino acid treatment, in
465 which it increased. This could be explained by two (non-exclusive) hypotheses: (1) amino acid
466 uptake and utilization, unlike glucose, does not undergo catabolite repression; (2) all of the
467 (dominant) bacteria in the community can take up and utilize amino acids. In support of the
468 second hypothesis, the genomes of more strains from the dominant bacteria in the mesocosms
469 contain pathways for the degradation of leucine compared to glucose (67±30% and 18±30%,
470 respectively, supplementary Table 6). Furthermore, it has been previously shown that more than
471 ~50% of bacterial cells take up leucin in different marine environments (Kirchman *et al.*, 1985),

472 compared with ~20% taking up glucose (Alonso and Pernthaler, 2005). Regardless of whether
473 amino acids do not undergo catabolite repression or are simply used by all the dominant bacteria,
474 these results provide further support that amino acids are common metabolic currencies in the
475 marine environment.

476

477 *Microbial interactions and competition- the 'big picture'*

478 Until now we have focused on the factors that determine whether an individual clade of bacteria
479 responds to the addition of different carbon source types. However, in experiments with natural
480 communities, interactions such as competition, allelopathy and syntrophy play a major role in
481 shaping microbial composition, influencing their metabolic activity (Orphan *et al.*, 2001; Morris
482 *et al.*, 2013; Corno *et al.*, 2015; Datta *et al.*, 2016), and thus the collective community function
483 (Fuhrman *et al.*, 2015; Graham *et al.*, 2016). For example, competition for the same molecular
484 classes and allelopathy, the process in which one organism produces compounds that influence
485 the growth and survival of another (Long and Azam, 2001), might explain the discrepancies
486 between the laboratory cultures (Forchielli *et al.*, 2022) and our microcosm experiment (see
487 further discussion in Supplementary Text 4). Indeed, all dominant families observed in our study
488 are able to produce anti-microbial compounds (Holmström, 1999; Lucas-Elio *et al.*, 2005;
489 Jeganathan *et al.*, 2013; Zoccarato *et al.*, 2022), but some seem to be more efficient competitors.
490 For example, a major inconsistency between the laboratory monocultures and mesocosms was
491 that *Alteromonadaceae* grew well in lab mono-cultures but became dominant in microcosms
492 only when disaccharides were added. In most other cases they were outcompeted by
493 *Vibrionaceae*. In a systematic analysis of antagonistic interacting between marine bacteria,
494 *Alteromonadaceae* and *Vibrionaceae* did not tent to inhibit one another (Long and Azam, 2001).

495 However, other studies suggest evidences for the competition between both families (Michotey
496 *et al.*, 2020), and for the advantage of *Vibrio* over *Alteromonas* when growing together on
497 different molecular classes (Eilers *et al.*, 2000). We speculate that only when *Alteromonadaceae*
498 had a clear metabolic advantage in the disaccharides treatment it was able to successfully
499 outcompete *Vibrionaceae*. Another case of potential allelopathy is between
500 *Pseudoalteromonadaceae* *Vibrionaceae* and *Alteromonadaceae* in the peptide treatment. As
501 mentioned above, all three families were able to grow on peptides in monocultures (Figure 5),
502 but when peptides were added to the EMS natural community *Pseudoalteromonadaceae* became
503 dominant (Figure 4C). Interestingly, two mechanisms by which *Pseudoalteromonas piscicida*
504 strains can kill different *Vibrionaceae* strains (including *Photobacterium*) were recently
505 identified: (1) secretion of antimicrobial substances and (2) direct transfer of apparently lytic
506 vesicles to the surface of competing bacteria, which causes the digestion of cell walls (Richards
507 *et al.*, 2017).

508

509 *Conclusions*

510 To what extent do heterotrophic bacteria differ in their ability to use the major macromolecular
511 blocks that comprise cell biomass, and that are released when cells die? In the specific
512 community tested here, from the ultra-oligotrophic EMS, amino acids seem to be a major driver
513 of heterotrophic growth. Amino acids induced the highest cell growth and activity (BP), and their
514 own uptake (as BP) was not inhibited by any other molecular class. In contrast, other molecular
515 classes induced less growth and lower activity, and the uptake of glucose was inhibited by other
516 molecular classes. Combining these bulk observations with measurements of 16S rRNA
517 expression suggests that that the overall community responses to different DOM components are

518 due to a complex interplay between changes at the scale of individual cells (e.g. catabolite
519 repression) and shifts in community composition. Assessing the growth of individual strains in
520 the lab on different molecular classes, and genomic analyses, provide only partial explanations to
521 the complex patterns exhibited when natural communities respond to different DOM sources.
522 This highlights the need to explore metabolism across more inter- and intra-clade diversity in
523 marine heterotrophic bacteria, possibly with the help of genome-scale models that can help
524 bridge lab experiments with ‘omics based field measurements.

525 **Acknowledgements**

526 We thank the captain and crew of the M/V Mediterranean Explorer for help during the cruise,
527 Tal Ben-Ezra and Mike Krom for the nutrient analyses and Yotam Fadida and Yoav Lehahn for
528 the satellite image. This study was supported by the Human Frontiers Science Program (grant
529 number grant RGP0020/2016, to DSh and DSe), the National Science Foundation - United
530 States-Israel Binational Science Foundation (NSFOCE-BSF 1635070 to DSe and Dsh), the Israel
531 Science foundation (grant 1786/20, to DS) and the Southern Marine Science and Engineering
532 Guangdong Laboratory (Guangzhou, grant SMSEGL20SC02, to DS). SG was supported by PhD
533 scholarships from the Yochai Bin Nun foundation (IOLR) and the University of Haifa. The work
534 of EF in Israel was supported by the Association for the Sciences of Limnology and
535 Oceanography (ASLO) LOREX fellowship, NSF-OISE no. 1831075

536

537 **References**

- 538 Alonso-Sáez, L., Sánchez, O., and Gasol, J.M. (2012) Bacterial uptake of low molecular weight organics
539 in the subtropical Atlantic: Are major phylogenetic groups functionally different? *Limnol Oceanogr*
540 **57**: 798–808.
- 541 Alonso, C. and Pernthaler, J. (2005) Incorporation of Glucose under Anoxic Conditions by
542 Bacterioplankton from Coastal North Sea Surface Waters. *Appl Environ Microbiol* **71**: 1709–1716.
- 543 Baltar, F., Lundin, D., Palovaara, J., Lekunberri, I., Reinthaler, T., Herndl, G.J., and Pinhassi, J. (2016)
544 Prokaryotic Responses to Ammonium and Organic Carbon Reveal Alternative CO₂ Fixation
545 Pathways and Importance of Alkaline Phosphatase in the Mesopelagic North Atlantic. *Front*
546 *Microbiol* **7**: 1–19.

- 547 Becker, J.W., Berube, P.M., Follett, C.L., Waterbury, J.B., Chisholm, S.W., DeLong, E.F., and Repeta,
548 D.J. (2014) Closely related phytoplankton species produce similar suites of dissolved organic
549 matter. *Front Microbiol* **5**: 1–14.
- 550 Biller, S.J., Schubotz, F., Roggensack, S.E., Thompson, A.W., Summons, R.E., and Chisholm, S.W.
551 (2014) Bacterial Vesicles in Marine Ecosystems. *Science* (80-) **343**: 183–186.
- 552 Bryson, S., Li, Z., Chavez, F., Weber, P.K., Pett-Ridge, J., Hettich, R.L., et al. (2017) Phylogenetically
553 conserved resource partitioning in the coastal microbial loop. *ISME J* **11**: 2781–2792.
- 554 Buchan, A., LeClerc, G.R., Gulvik, C.A., and González, J.M. (2014) Master recyclers: features and
555 functions of bacteria associated with phytoplankton blooms. *Nat Rev Microbiol* **12**: 686–698.
- 556 Callahan, B.J., McMurdie, P.J., Rosen, M.J., Han, A.W., Johnson, A.J.A., and Holmes, S.P. (2016)
557 DADA2: High-resolution sample inference from Illumina amplicon data. *Nat Methods* **13**: 581–583.
- 558 Cembella, A. D., Antia, N. J., & Harrison, P.J. (1982) The utilization of inorganic and organic
559 phosphorous compounds as nutrients by eukaryotic microalgae: A multidisciplinary perspective:
560 Part I. *CRC Crit Rev Microbiol* **10**: 317–391.
- 561 Church, M.J., Hutchins, D.A., and Ducklow, H.W. (2000) Limitation of Bacterial Growth by Dissolved
562 Organic Matter and Iron in the Southern Ocean. *Appl Environ Microbiol* **66**: 455–466.
- 563 Corno, G., Salka, I., Pohlmann, K., Hall, A., and Grossart, H. (2015) Interspecific interactions drive chitin
564 and cellulose degradation by aquatic microorganisms. *Aquat Microb Ecol* **76**: 27–37.
- 565 Cude, W.N., Mooney, J., Tavanaei, A.A., Hadden, M.K., Frank, A.M., Gulvik, C.A., et al. (2012)
566 Production of the Antimicrobial Secondary Metabolite Indigoidine Contributes to Competitive
567 Surface Colonization by the Marine Roseobacter *Phaeobacter* sp. Strain Y4I. *Appl Environ*
568 *Microbiol* **78**: 4771–4780.
- 569 D’Souza, G., Shitut, S., Preussger, D., Yousif, G., Waschina, S., and Kost, C. (2018) Ecology and

- 570 evolution of metabolic cross-feeding interactions in bacteria. *Nat Prod Rep* **35**: 455–488.
- 571 Datta, M.S., Sliwerska, E., Gore, J., Polz, M.F., and Cordero, O.X. (2016) Microbial interactions lead to
572 rapid micro-scale successions on model marine particles. *Nat Commun* **7**: 11965.
- 573 Dittmar T, A.C. (2018) An inseparable liaison: marine microbes and nonliving organic matter. In
574 *Microbial ecology of the oceans*. Gasol JM, K.D. (ed). Hoboken, NJ: John Wiley & Sons, pp. 195–
575 229.
- 576 Dyhrman, S.T., Chappell, P.D., Haley, S.T., Moffett, J.W., Orchard, E.D., Waterbury, J.B., and Webb,
577 E.A. (2006) Phosphonate utilization by the globally important marine diazotroph *Trichodesmium*.
578 *Nature* **439**: 68–71.
- 579 Eigemann, F., Rahav, E., Grossart, H., Aharonovich, D., Sher, D., Vogts, A., and Voss, M. (2022)
580 Phytoplankton exudates provide full nutrition to a subset of accompanying heterotrophic bacteria via
581 carbon, nitrogen and phosphorus allocation. *Environ Microbiol* **24**: 2467–2483.
- 582 Eilers, H., Pernthaler, J., and Amann, R. (2000) Succession of Pelagic Marine Bacteria during
583 Enrichment: a Close Look at Cultivation-Induced Shifts. *Appl Environ Microbiol* **66**: 4634–4640.
- 584 Ben Ezra, T., Krom, M.D., Tsemel, A., Berman-Frank, I., Herut, B., Lehahn, Y., et al. (2021) Seasonal
585 nutrient dynamics in the P depleted Eastern Mediterranean Sea. *Deep Sea Res Part I Oceanogr Res*
586 *Pap* **176**: 103607.
- 587 Fandino, L., Riemann, L., Steward, G., Long, R., and Azam, F. (2001) Variations in bacterial community
588 structure during a dinoflagellate bloom analyzed by DGGE and 16S rDNA sequencing. *Aquat*
589 *Microb Ecol* **23**: 119–130.
- 590 Feingersch, R., Filosof, A., Mejuch, T., Glaser, F., Alalouf, O., Shoham, Y., and Béjà, O. (2012)
591 Potential for phosphite and phosphonate utilization by *Prochlorococcus*. *ISME J* **6**: 827–834.
- 592 Ferrer-González, F.X., Widner, B., Holderman, N.R., Glushka, J., Edison, A.S., Kujawinski, E.B., and

- 593 Moran, M.A. (2021) Resource partitioning of phytoplankton metabolites that support bacterial
594 heterotrophy. *ISME J* **15**: 762–773.
- 595 Finkel, Z. V., Follows, M.J., Liefer, J.D., Brown, C.M., Benner, I., and Irwin, A.J. (2016) Phylogenetic
596 diversity in the macromolecular composition of microalgae. *PLoS One* **11**:
- 597 Forchielli, E., Sher, D., & Segrè, D. (2022) Metabolic phenotyping of marine heterotrophs on refactored
598 media reveals diverse metabolic adaptations and lifestyle strategies. *Msystems* **7**: e00070-22.
- 599 Fuhrman, J.A., Cram, J.A., and Needham, D.M. (2015) Marine microbial community dynamics and their
600 ecological interpretation. *Nat Rev Microbiol* **13**: 133–146.
- 601 Geider, R.J. and La Roche, J. (2002) Redfield revisited: Variability of C:N:P in marine microalgae and its
602 biochemical basis. *Eur J Phycol* **37**: 1–17.
- 603 Gómez-Consarnau, L., Lindh, M. V., Gasol, J.M., and Pinhassi, J. (2012) Structuring of bacterioplankton
604 communities by specific dissolved organic carbon compounds. *Environ Microbiol* **14**: 2361–2378.
- 605 Graham, E.B., Knelman, J.E., Schindlbacher, A., Siciliano, S., Breulmann, M., Yannarell, A., et al.
606 (2016) Microbes as Engines of Ecosystem Function: When Does Community Structure Enhance
607 Predictions of Ecosystem Processes? *Front Microbiol* **7**: 1–10.
- 608 Haber, M., Roth Rosenberg, D., Lalzar, M., Burgsdorf, I., Saurav, K., Lionheart, R., et al. (2022)
609 Spatiotemporal Variation of Microbial Communities in the Ultra-Oligotrophic Eastern
610 Mediterranean Sea. *Front Microbiol* **13**:
- 611 Hadley Wickham, Romain François, Lionel Henry, K.M. and D.V. (2023) dplyr: A Grammar of Data
612 Manipulation.
- 613 Haider, M.N., Iqbal, M.M., Nishimura, M., Ikemoto, E., Ijichi, M., and Kogure, K. (2023) Bacterial
614 response to glucose addition: growth and community structure in seawater microcosms from North
615 Pacific Ocean. *Sci Rep* **13**: 341.

- 616 Hertkorn, N., Harir, M., Koch, B.P., Michalke, B., and Schmitt-Kopplin, P. (2013) High-field NMR
617 spectroscopy and FTICR mass spectrometry: powerful discovery tools for the molecular level
618 characterization of marine dissolved organic matter. *Biogeosciences* **10**: 1583–1624.
- 619 Holmström, C. (1999) Marine Pseudoalteromonas species are associated with higher organisms and
620 produce biologically active extracellular agents. *FEMS Microbiol Ecol* **30**: 285–293.
- 621 Jari Oksanen, Gavin L. Simpson, F. Guillaume Blanchet, Roeland Kindt, P., Legendre, Peter R. Minchin,
622 R.B. O’Hara, Peter Solymos, M.H.H.S., Eduard Szoecs, Helene Wagner, Matt Barbour, Michael
623 Bedward, B.B., Daniel Borcard, Gustavo Carvalho, Michael Chirico, M.D.C., Sebastien Durand,
624 Heloisa Beatriz Antoniazi Evangelista, R.F., Michael Friendly, Brendan Furneaux, Geoffrey
625 Hannigan, Mark O. Hill, L., et al. (2022) vegan: Community Ecology Package.
- 626 Jeganathan, P., Rajasekaran, K.M., Asha Devi, N.K., and Karuppusamy, S. (2013) Antimicrobial activity
627 and Characterization of Marine bacteria. *Indian J Pharm Biol Res* **1**: 38–44.
- 628 Kassambara, A. (2023a) ggpubr: “ggplot2” Based Publication Ready Plots.
- 629 Kassambara, A. (2023b) rstatix: Pipe-Friendly Framework for Basic Statistical Tests.
- 630 Keil, R. and Kirchman, D. (1991) Contribution of dissolved free amino acids and ammonium to the
631 nitrogen requirements of heterotrophic bacterioplankton. *Mar Ecol Prog Ser* **73**: 1–10.
- 632 Keller, L. and Surette, M.G. (2006) Communication in bacteria: an ecological and evolutionary
633 perspective. *Nat Rev Microbiol* **4**: 249–258.
- 634 Kharbush, J.J., Close, H.G., Van Mooy, B.A.S., Arnosti, C., Smittenberg, R.H., Le Moigne, F.A.C., et al.
635 (2020) Particulate Organic Carbon Deconstructed: Molecular and Chemical Composition of
636 Particulate Organic Carbon in the Ocean. *Front Mar Sci* **7**: 1–10.
- 637 Kirchman, D., K’nees, E., and Hodson, R. (1985) Leucine incorporation and its potential as a measure of
638 protein synthesis by bacteria in natural aquatic systems. *Appl Environ Microbiol* **49**: 599–607.

- 639 Kirchman, D.L., Meon, B., Cottrell, M.T., Hutchins, D.A., Weeks, D., and Bruland, K.W. (2000) Carbon
640 versus iron limitation of bacterial growth in the California upwelling regime. *Limnol Oceanogr* **45**:
641 1681–1688.
- 642 Koch, H., Dürwald, A., Schweder, T., Noriega-Ortega, B., Vidal-Melgosa, S., Hehemann, J.-H., et al.
643 (2019) Biphasic cellular adaptations and ecological implications of *Alteromonas macleodii*
644 degrading a mixture of algal polysaccharides. *ISME J* **13**: 92–103.
- 645 Konopka, J.B. (2012) N-Acetylglucosamine Functions in Cell Signaling. *Scientifica (Cairo)* **2012**: 1–15.
- 646 Kuhlisch, C., Schleyer, G., Shahaf, N., Vincent, F., Schatz, D., and Vardi, A. (2021) Viral infection of
647 algal blooms leaves a unique metabolic footprint on the dissolved organic matter in the ocean. *Sci*
648 *Adv* **7**: 1–14.
- 649 Larsson, U. and Hagström, A. (1979) Phytoplankton exudate release as an energy source for the growth of
650 pelagic bacteria. *Mar Biol* **52**: 199–206.
- 651 Long, R.A. and Azam, F. (2001) Antagonistic Interactions among Marine Pelagic Bacteria. *Appl Environ*
652 *Microbiol* **67**: 4975–4983.
- 653 Lopez, J.S., Garcia, N.S., Talmy, D., and Martiny, A.C. (2016) Diel variability in the elemental
654 composition of the marine cyanobacterium *synechococcus*. *J Plankton Res* **38**: 1052–1061.
- 655 Lucas-Elio, P., Hernandez, P., Sanchez-Amat, A., and Solano, F. (2005) Purification and partial
656 characterization of marinocine, a new broad-spectrum antibacterial protein produced by
657 *Marinomonas mediterranea*. *Biochim Biophys Acta - Gen Subj* **1721**: 193–203.
- 658 Lyons, M.M., Lau, Y.-T., Carden, W.E., Ward, J.E., Roberts, S.B., Smolowitz, R., et al. (2007)
659 Characteristics of Marine Aggregates in Shallow-water Ecosystems: Implications for Disease
660 Ecology. *Ecohealth* **4**: 406–420.
- 661 Martin-Platero, A.M., Cleary, B., Kauffman, K., Preheim, S.P., McGillicuddy, D.J., Alm, E.J., and Polz,

- 662 M.F. (2018) High resolution time series reveals cohesive but short-lived communities in coastal
663 plankton. *Nat Commun* **9**: 266.
- 664 Mary, I., Tarran, G.A., Warwick, P.E., Terry, M.J., Scanlan, D.J., Burkill, P.H., and Zubkov, M. V.
665 (2008) Light enhanced amino acid uptake by dominant bacterioplankton groups in surface waters of
666 the Atlantic Ocean. *FEMS Microbiol Ecol* **63**: 36–45.
- 667 Michotey, V., Blanfuné, A., Chevalier, C., Garel, M., Diaz, F., Berline, L., et al. (2020) In situ
668 observations and modelling revealed environmental factors favouring occurrence of *Vibrio* in
669 microbiome of the pelagic Sargassum responsible for strandings. *Sci Total Environ* **748**: 141216.
- 670 Middelboe, M., Borch, N., and Kirchman, D. (1995) Bacterial utilization of dissolved free amino acids,
671 dissolved combined amino acids and ammonium in the Delaware Bay estuary: effects of carbon and
672 nitrogen limitation. *Mar Ecol Prog Ser* **128**: 109–120.
- 673 Møller, E., Thor, P., and Nielsen, T. (2003) Production of DOC by *Calanus finmarchicus*, *C. glacialis* and
674 *C. hyperboreus* through sloppy feeding and leakage from fecal pellets. *Mar Ecol Prog Ser* **262**: 185–
675 191.
- 676 Møller, E.F. (2007) Production of dissolved organic carbon by sloppy feeding in the copepods *Acartia*
677 *tonsa*, *Centropages typicus*, and *Temora longicornis*. *Limnol Oceanogr* **52**: 79–84.
- 678 Moran, M.A., Ferrer-González, F.X., Fu, H., Nowinski, B., Olofsson, M., Powers, M.A., et al. (2022) The
679 Ocean's labile DOC supply chain. *Limnol Oceanogr* **67**: 1007–1021.
- 680 Moran, M.A., Kujawinski, E.B., Stubbins, A., Fatland, R., Aluwihare, L.I., Buchan, A., et al. (2016)
681 Deciphering ocean carbon in a changing world. *Proc Natl Acad Sci U S A* **113**: 3143–3151.
- 682 Morris, B.E.L., Henneberger, R., Huber, H., and Moissl-Eichinger, C. (2013) Microbial syntrophy:
683 interaction for the common good. *FEMS Microbiol Rev* **37**: 384–406.
- 684 Munson-McGee, J.H., Lindsay, M.R., Sintes, E., Brown, J.M., D'Angelo, T., Brown, J., et al. (2022)

- 685 Decoupling of respiration rates and abundance in marine prokaryoplankton. *Nature* **612**: 764–770.
- 686 Orphan, V.J., House, C.H., Hinrichs, K.-U., McKeegan, K.D., and DeLong, E.F. (2001) Methane-
687 Consuming Archaea Revealed by Directly Coupled Isotopic and Phylogenetic Analysis. *Science*
688 (80-) **293**: 484–487.
- 689 Pinhassi, J., Sala, M.M., Havskum, H., Peters, F., Guadayol, Ò., Malits, A., and Marrasé, C. (2004)
690 Changes in Bacterioplankton Composition under Different Phytoplankton Regimens. *Appl Environ*
691 *Microbiol* **70**: 6753–6766.
- 692 Pontiller, B., Martínez-García, S., Lundin, D., and Pinhassi, J. (2020) Labile Dissolved Organic Matter
693 Compound Characteristics Select for Divergence in Marine Bacterial Activity and Transcription.
694 *Front Microbiol* **11**: 1–19.
- 695 Quast, C., Pruesse, E., Yilmaz, P., Gerken, J., Schweer, T., Yarza, P., et al. (2012) The SILVA ribosomal
696 RNA gene database project: improved data processing and web-based tools. *Nucleic Acids Res* **41**:
697 D590–D596.
- 698 R Development Core Team, R.F.F.S.C. (2011) R: A language and environment for statistical computing.
- 699 Rahav, E., Silverman, J., Raveh, O., Hazan, O., Rubin-Blum, M., Zeri, C., et al. (2019) The deep water of
700 Eastern Mediterranean Sea is a hotspot for bacterial activity. *Deep Sea Res Part II Top Stud*
701 *Oceanogr* **164**: 135–143.
- 702 Reich, T., Ben-Ezra, T., Belkin, N., Tsemel, A., Aharonovich, D., Roth-Rosenberg, D., et al. (2022) A
703 year in the life of the Eastern Mediterranean: Monthly dynamics of phytoplankton and
704 bacterioplankton in an ultra-oligotrophic sea. *Deep Sea Res Part I Oceanogr Res Pap* **182**: 103720.
- 705 Rich, J.H., Ducklow, H.W., and Kirchman, D.L. (1996) Concentrations and uptake of neutral
706 monosaccharides along 14°W in the equatorial Pacific: Contribution of glucose to heterotrophic
707 bacterial activity and the DOM flux. *Limnol Oceanogr* **41**: 595–604.

- 708 Richards, G.P., Watson, M.A., Needleman, D.S., Uknalis, J., Boyd, E.F., and Fay, P. (2017) Mechanisms
709 for *Pseudoalteromonas piscicida*-induced killing of vibrios and other bacterial pathogens. *Environ*
710 *Microbiol* **83**: 1–17.
- 711 Riemann, L. and Azam, F. (2002) Widespread N -Acetyl- d -Glucosamine Uptake among Pelagic Marine
712 Bacteria and Its Ecological Implications. *Appl Environ Microbiol* **68**: 5554–5562.
- 713 Riemann, L., Steward, G.F., and Azam, F. (2000) Dynamics of Bacterial Community Composition and
714 Activity during a Mesocosm Diatom Bloom. *Appl Environ Microbiol* **66**: 2282–2282.
- 715 Rinta-Kanto, J.M., Sun, S., Sharma, S., Kiene, R.P., and Moran, M.A. (2012) Bacterial community
716 transcription patterns during a marine phytoplankton bloom. *Environ Microbiol* **14**: 228–239.
- 717 Roth-Rosenberg, D., Aharonovich, D., Omta, A.W., Follows, M.J., and Sher, D. (2021) Dynamic
718 macromolecular composition and high exudation rates in *Prochlorococcus*. *Limnol Oceanogr* **66**:
719 1759–1773.
- 720 Roth Rosenberg, D., Haber, M., Goldford, J., Lalzar, M., Aharonovich, D., Al-Ashhab, A., ... & Sher, D.
721 (2021) Particle-associated and free-living bacterial communities in an oligotrophic sea are affected
722 by different environmental factors. *Environ Microbiol* **23**: 4295–4308.
- 723 Ruiz-González, C., Galí, M., Gasol, J.M., and Simó, R. (2012) Sunlight effects on the DMSP-sulfur and
724 leucine assimilation activities of polar heterotrophic bacterioplankton. *Biogeochemistry* **110**: 57–74.
- 725 Salazar, G., Paoli, L., Alberti, A., Huerta-Cepas, J., Ruscheweyh, H.-J., Cuenca, M., et al. (2019) Gene
726 Expression Changes and Community Turnover Differentially Shape the Global Ocean
727 Metatranscriptome. *Cell* **179**: 1068-1083.e21.
- 728 Sarmiento, H. and Gasol, J.M. (2012) Use of phytoplankton-derived dissolved organic carbon by different
729 types of bacterioplankton. *Environ Microbiol* **14**: 2348–2360.
- 730 Sarmiento, H., Morana, C., and Gasol, J.M. (2016) Bacterioplankton niche partitioning in the use of

- 731 phytoplankton-derived dissolved organic carbon: quantity is more important than quality. *ISME J*
732 **10**: 2582–2592.
- 733 Schlesinger, W. H., & Bernhardt, E.S. (2013) Biogeochemistry: an analysis of global change, Academic
734 press.
- 735 Schwalbach, M.S., Tripp, H.J., Steindler, L., Smith, D.P., and Giovannoni, S.J. (2010) The presence of
736 the glycolysis operon in SAR11 genomes is positively correlated with ocean productivity. *Environ*
737 *Microbiol* **12**: 490–500.
- 738 Sebastián, M., Pitta, P., González, J.M., Thingstad, T.F., and Gasol, J.M. (2012) Bacterioplankton groups
739 involved in the uptake of phosphate and dissolved organic phosphorus in a mesocosm experiment
740 with P-starved Mediterranean waters. *Environ Microbiol* **14**: 2334–2347.
- 741 Simon, M. and Azam, F. (1989) Protein content and protein synthesis rates of planktonic marine bacteria.
742 *Mar Ecol Prog Ser* **51**: 201–213.
- 743 Skoog, A., Biddanda, B., and Benner, R. (1999) Bacterial utilization of dissolved glucose in the upper
744 water column of the Gulf of Mexico. *Limnol Oceanogr* **44**: 1625–1633.
- 745 Sosa, O.A., Gifford, S.M., Repeta, D.J., and DeLong, E.F. (2015) High molecular weight dissolved
746 organic matter enrichment selects for methylotrophs in dilution to extinction cultures. *ISME J* **9**:
747 2725–2739.
- 748 Sosa, O.A., Repeta, D.J., DeLong, E.F., Ashkezari, M.D., and Karl, D.M. (2019) Phosphate-limited ocean
749 regions select for bacterial populations enriched in the carbon–phosphorus lyase pathway for
750 phosphonate degradation. *Environ Microbiol* **21**: 2402–2414.
- 751 Spencer Graves, Hans-Peter Piepho, L.S. with help from S.D.-R. (2019) multcompView: Visualizations
752 of Paired Comparisons.
- 753 Summons, R.E. (1993) Biogeochemical cycles. In *Organic geochemistry*. pp. 3–21.

- 754 Takemura, A.F., Chien, D.M., and Polz, M.F. (2014) Associations and dynamics of Vibrionaceae in the
755 environment, from the genus to the population level. *Front Microbiol* **5**: 1–26.
- 756 Tang, B.-L., Yang, J., Chen, X.-L., Wang, P., Zhao, H.-L., Su, H.-N., et al. (2020) A predator-prey
757 interaction between a marine *Pseudoalteromonas* sp. and Gram-positive bacteria. *Nat Commun* **11**:
758 285.
- 759 Team, R. (2020) RStudio: integrated development for R. RStudio, PBC.
- 760 Teeling, H., Fuchs, B.M., Becher, D., Klockow, C., Gardebrecht, A., Bennke, C.M., et al. (2012)
761 Substrate-Controlled Succession of Marine Bacterioplankton Populations Induced by a
762 Phytoplankton Bloom. *Science (80-)* **336**: 608–611.
- 763 Thingstad, T.F. and Mantoura, R.F.C. (2005) Titrating excess nitrogen content of phosphorous-deficient
764 eastern Mediterranean surface water using alkaline phosphatase activity as a bio-indicator. *Limnol*
765 *Oceanogr Methods* **3**: 94–100.
- 766 Thornton, D.C.O. (2014) Dissolved organic matter (DOM) release by phytoplankton in the contemporary
767 and future ocean. *Eur J Phycol* **49**: 20–46.
- 768 Tinta, T., Zhao, Z., Bayer, B., and Herndl, G.J. (2023) Jellyfish detritus supports niche partitioning and
769 metabolic interactions among pelagic marine bacteria. *Microbiome* **11**: 156.
- 770 Vargas, M.A., Rodríguez, H., Moreno, J., Olivares, H., Del Campo, J.A., Rivas, J., and Guerrero, M.G.
771 (1998) Biochemical composition and fatty acid content of filamentous nitrogen-fixing
772 cyanobacteria. *J Phycol* **34**: 812–817.
- 773 Walters, W., Hyde, E.R., Berg-lyons, D., Ackermann, G., Humphrey, G., Parada, A., et al. (2015)
774 Transcribed Spacer Marker Gene Primers for Microbial Community Surveys. *mSystems* **1**: e0009-
775 15.
- 776 Weinbauer, M.G. (2004) Ecology of prokaryotic viruses. *FEMS Microbiol Rev* **28**: 127–181.

- 777 Wickham, H., Averick, M., Bryan, J., Chang, W., McGowan, L., François, R., Grolemund, G., Hayes, A.,
778 Henry, L., Hester, J., Kuhn, M., Pedersen, T., Miller, E., Bache, S., Müller, K., Ooms, J., Robinson,
779 D., Seidel, D., Spinu, V., ... Yutani, H. Wickham, H., H. (2019) Welcome to the tidyverse. *J Open*
780 *Source Softw* **4**: 1686.
- 781 Wickham, H. (2016) ggplot2: Elegant Graphics for Data Analysis.
- 782 Zhang, X., Lin, H., Wang, X., and Austin, B. (2018) Significance of *Vibrio* species in the marine organic
783 carbon cycle—A review. *Sci China Earth Sci* **61**: 1357–1368.
- 784 Zhao, H.L., Chen, X.L., Xie, B. Bin, Zhou, M.Y., Gao, X., Zhang, X.Y., et al. (2012) Elastolytic
785 mechanism of a novel M23 metalloprotease pseudoalterin from deep-sea *Pseudoalteromonas* sp.
786 CF6-2: Cleaving not only glycyl bonds in the hydrophobic regions but also peptide bonds in the
787 hydrophilic regions involved in cross-linking. *J Biol Chem* **287**: 39710–39720.
- 788 Zoccarato, L., Sher, D., Miki, T., Segrè, D., and Grossart, H.-P. (2022) A comparative whole-genome
789 approach identifies bacterial traits for marine microbial interactions. *Commun Biol* **5**: 276.
- 790 Zubkov, M. V., Tarran, G.A., Mary, I., and Fuchs, B.M. (2008) Differential microbial uptake of dissolved
791 amino acids and amino sugars in surface waters of the Atlantic Ocean. *J Plankton Res* **30**: 211–220.
- 792